The PBPK LeiCNS-PK3.0 framework predicts Nirmatrelvir (but not Remdesivir or Molnupiravir) to achieve effective concentrations against SARS-CoV-2 in human brain cells

Saleh, M.A.A.E.W.; Hirasawa, M.; Sun, M.; Berfin, G.; Elassaiss, J.; Lange, E.C.M. de

The PBPK LeiCNS-PK3.0 framework predicts Nirmatrelvir (but not Remdesivir or Molnupiravir) to achieve effective concentrations against SARS-CoV-2 in human brain cells

Mohammed A.A. Saleh , Makoto Hirasawa , Ming Sun ,
Berfin Gülave , Jeroen Elassaiss-Schaap ,
Elizabeth C.M. de Lange

PII: S0928-0987(22)00230-5
DOI: https://doi.org/10.1016/j.ejps.2022.106345
Reference: PHASCI 106345

To appear in: *European Journal of Pharmaceutical Sciences*

Received date: 3 August 2022
Revised date: 17 November 2022
Accepted date: 29 November 2022

The PBPK LeiCNS-PK3.0 framework predicts Nirmatrelvir (but not Remdesivir or Molnupiravir) to achieve effective concentrations against SARS-CoV-2 in human brain cells

Mohammed A. A. Saleh[1], Makoto Hirasawa[2], Ming Sun[3], Berfin Gülave[4], Jeroen Elassaiss-Schaap[5], Elizabeth C. M. de Lange[6]

[1]Division of Systems Pharmacology and Pharmacy, Leiden Academic Center for Drug Research, Leiden University, Leiden, The Netherlands. ORCID ID: 0000-0002-0517-6051

[2]Division of Systems Pharmacology and Pharmacy, Leiden Academic Center for Drug Research, Leiden University, Leiden, The Netherlands. ORCID ID: 0000-0002-1678-8539

[3]Division of Systems Pharmacology and Pharmacy, Leiden Academic Center for Drug Research, Leiden University, Leiden, The Netherlands. ORCID ID: 0000-0001-8018-1152

[4]Division of Systems Pharmacology and Pharmacy, Leiden Academic Center for Drug Research, Leiden University, Leiden, The Netherlands. ORCID ID: 0000-0001-8954-882X

[5]PD-value B.V., Houten, The Netherlands. ORCID ID: 0000-0002-3333-861X

[6]Division of Systems Pharmacology and Pharmacy, Leiden Academic Center for Drug Research, Leiden University, Leiden, The Netherlands. ORCID ID: 0000-0001-8303-1117

[*]Correspondence: Dr. Elizabeth CM De Lange, Leiden University Leiden Academic Centre for Drug Research, Netherlands, ecmdelange@lacdr.leidenuniv.nl, telephone: +31 71 527 6330, address: Gorlaeus laboratorium, Einsteinweg 55, 2333 CC, Leiden, The Netherlands

Graphical abstract

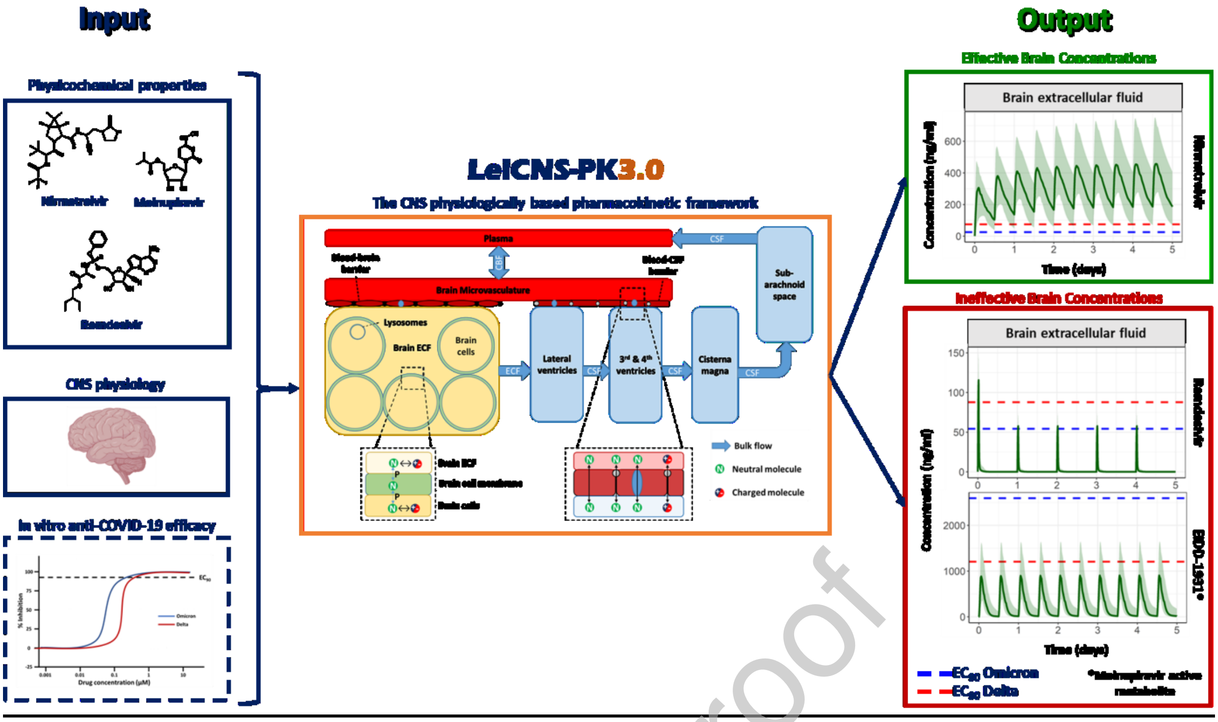

Highlights

- No information exists on the pharmacokinetics of antiCOVID-19 drugs in human brain
- LeiCNS-PK3.0 framework predicts adequately the human brain pharmacokinetic profiles
- Nirmatrelvir is predicted to reach effective brain concentrations against COVID-19
- Ineffective brain concentrations are predicted for Molnupiravir and Remdesivir
- LeiCNS-PK3.0 is a promising tool to optimize and accelerate CNS drug development

Abstract

SARS-CoV-2 was shown to infect and persist in the human brain cells up to 230 days, highlighting the need to treat the brain viral load. The CNS disposition of antiCOVID-19 drugs: Remdesivir, Molnupiravir, and Nirmatrelvir, remains, however, unexplored. Here, we assessed the human brain pharmacokinetic profile (PK) against the EC_{90} values of antiCOVID-19 drugs to predict drugs with favorable brain PK against the delta and omicron variants. We also evaluated the intracellular PK of GS443902 and EIDD2061, the active metabolites of Remdesivir and Molnupiravir. Towards this, we applied LeiCNS-PK3.0, the physiologically based pharmacokinetic framework with demonstrated adequate predictions of human CNS PK. Under the recommended dosing regimens, the predicted brain extracellular fluid PK of only Nirmatrelvir was above the variants' EC_{90}. The intracellular levels of GS443902 and EIDD2061 were below the intracellular EC_{90}.

Summarizing, our model recommends Nirmatrelvir as the promising candidate for (pre)clinical studies investigating the CNS efficacy of antiCOVID-19 drugs.

***Keywords**:* LeiCNS-PK3.0, COVID-19, brain, pharmacokinetics

1. Introduction

Increasing evidence supports that COVID-19 is not only a respiratory disease but may also have serious impact on, among others, the central nervous system (CNS) (Philippens et al., 2021). The neurological manifestations associated with SARS-CoV-2 include headaches, encephalopathy (Chou et al., 2021; Guadarrama-Ortiz et al., 2020), Alzheimer's disease-like manifestations (Shen et al., 2022), and brain atrophy (Douaud et al., 2022). SARS-CoV-2 has also been demonstrated to infect (Matschke et al., 2020; Veleri, 2022) and persist in neurons for up to 230 days (Stein et al., 2021). A causal relationship of neurotropism and neurological manifestations is still, however, unestablished (Pacheco-Herrero et al., 2021; Shen et al., 2022; Yang et al., 2021). Addressing the viral infection in the brain is therefore relevant to avoid a long-term latent state of virus in the CNS, which could result in recurrent CNS pathologies.

Three small molecule drugs have so far been approved for the treatment of COVID-19 in humans, which include the main protease inhibitor, Nirmatrelvir, in addition to Remdesivir and Molnupiravir that are activated intracellularly to the nucleoside analogues GS443902 and EIDD2061, respectively. The PK profiles of these drugs and their active metabolites in the human brain have not been assessed. We here apply the physiologically based LeiCNS-PK3.0 framework to predict the PK profiles of these drugs in the brain, and relate these to their in vitro EC_{90} (Gonçalves et al., 2020) values against the delta and omicron variants of SARS-CoV-2. By this approach we select drug(s) that seems to be promising for treating these viruses in the brain.

2. Data and Methods

2.1. Data collection

We first compiled in vitro and preclinical in vivo data on CNS disposition and blood-brain barrier (BBB) transport of Nirmatrelvir, Remdesivir (and its metabolites: GS704277, GS441524, and its active form GS443902), and Molnupiravir (and its metabolites: EIDD1931 and its active form EIDD2061). Molnupiravir is unstable in plasma and is efficiently and rapidly converted to EIDD1931. Therefore, EIDD1931 was used as a surrogate to describe Molnupiravir's plasma and CNS disposition. Also, Molnupiravir dosing was performed in molarity to account for the difference in molecular weight between the parent drug and its metabolite.

In addition, the extent of CNS distribution of these drugs given by $Kp_{uu,BBB}$ (brain$_{ECF}$ to plasma unbound drug ratio) was evaluated using the in-silico brain exposure efficiency (BEE) score (Gupta et al., 2020). Population plasma PK models were extracted from literature. Drug physicochemical properties were available from DRUGBANK (Wishart et al., 2017). The model related input is reported in table 1. Literature data, where required, were digitized with WebPlotDigitizer version 4.2 (https://apps.automeris.io/wpd/).

2.2. LeiCNS-PK3.0 framework

LeiCNS-PK3.0 is a physiologically based pharmacokinetic (PBPK) model of the CNS, which can predict the unbound PK profile in different CNS compartments, including the target sites in the brain extracellular (brain$_{ECF}$) and intracellular (brain$_{ICF}$) compartments and also the lumbar cerebrospinal fluid compartment. The model was previously validated and was shown to predict, independently of clinical brain PK data, the unbound PK profiles of morphine in the human brain$_{ECF}$ and of indomethacin, oxycodone, and acetaminophen at the lumbar region of the subarachnoid space cerebrospinal fluid (CSF) compartments, both with less than two-fold error. Additional details on model structure and validation have been reported previously (Saleh et al., 2021). Here, we will use the validated LeiCNS-PK3.0 to predict the human brain$_{ECF}$ and brain$_{ICF}$ PK profiles of the three antiCOVID-19 drugs. It will not be possible, however, to validate these predictions since relevant brain PK measurements are unavailable.

2.3. LeiCNS-PK3.0 simulations

Model simulations were performed using the physiological parameters of a healthy human adult as reported previously (Saleh et al., 2021) and the plasma PK parameters and drug physicochemical properties presented in table 1. Fifty simulations were performed to account for interindividual variability of the population plasma PK models and the median and 95 percentiles were reported. Simulations were performed in R (version 4.1.2) (R Core Team, 2019) using the package RxODE (version 1.1.4) (Fidler et al., 2019) and the LSODA (Livermore Solver for Ordinary Differential Equations) Fortran package.

2.4. Brain intracellular PK assessment

Remdesivir is a prodrug and is metabolized intracellularly to GS443902, the active nucleoside analogue. GS443902 is hydrophilic, with long elimination half-life (≈ 43 hours) as measured in human PBMCs (Humeniuk et al., 2021), which imply that GS443902 may accumulate intracellularly, producing a sustained effect. We therefore investigated the intracellular brain PK profile of GS443902. The intracellular PK profiles of

Remdesivir metabolites were reported in lung epithelium cells (Calu-3 cells) (Gilead Sciences, 2020) and were used to model the intracellular brain PK of GS443902. Briefly, we assumed that the triphosphate active metabolite GS443902 is formed from GS704277 metabolite directly (half-life = 30.4 hours), given the low concentrations of the intermediate monophosphate and diphosphate metabolites. The formation rate of GS443902 was multiplied by a factor of 24.9 to correct for the slow metabolic rate of Calu-3 cell line compared to other human cell lines, for example the hepatocellular carcinoma (Huh-7), primary airway epithelium (HAE), and kidney epithelium (293T) (Pruijssers et al., 2020; Tao et al., 2021). No formation of GS443902 from GS441524 was considered, supported by the inefficiency of this process, as demonstrated by the in vitro experiments using the Huh-7, HAE, Calu-3, Caco-2, and 293T cell lines (Gilead Sciences, 2020; Tao et al., 2021). GS443902 is metabolized to GS441524 with a half-life of 43 hours (Humeniuk et al., 2021).

Likewise, Molnupiravir is the prodrug of the parent nucleoside EIDD1931, which undergoes intracellular conversion to EIDD2061, the triphosphate metabolite of EIDD1931. Intracellular PK of EIDD2061 was modeled based on the mouse brain homogenate data of EIDD1931 and EIDD2061 (Painter et al., 2019). The formation and elimination half-lives of EIDD2061 were 3.5 (Painter et al., 2019) and 4.5 (European Medicines Agency, 2021a) hours, respectively.

2.5. Efficacy calculation

Comparison of predicted brain$_{ECF}$ PK profile against the EC_{90} was used to assess if a drug would achieve effective brain PK. Efficacy against the omicron and delta variants was considered as these are the current variants of concern (World Health Organization (WHO), n.d.). In addition, efficacy at a given time point (ε_t) was calculated using the predicted brain$_{ECF}$ concentrations at given time point ($C_{ECF,t}$) and EC_{50}. Average efficacy (ε) of the drug across the PK profile was calculated by integrating ε_t over the treatment duration (D) (Gonçalves et al., 2020). In vitro measured EC_{50} and EC_{90} were available from literature and are reported in table 1.

$$\varepsilon_t = \frac{C_{ECF,t}}{EC_{50} + C_{ECF,t}}$$

$$\varepsilon = \frac{1}{D} * \int_0^D \varepsilon_t \, dt$$

2.6. Sensitivity analysis

A sensitivity analysis was performed to evaluate the impact of the CNS pathophysiological changes associated with COVID-19 on brain PK profiles of the three antiCOVID-19 drugs (Saleh and de Lange, 2021). Changes of all model physiological parameters were assessed including pH values of $brain_{ECF}$, $brain_{ICF}$, lysosomes, plasma, and CSF; effective surface area of paracellular transport across the BBB and blood-CSF (BCSFB); bulk fluid flow as cerebral blood flow, $brain_{ECF}$ bulk flow, and CSF flow; surfaces areas of BBB, BCSFB, brain cells, and lysosomes; and the volumes of brain microvasculature, $brain_{ECF}$, $brain_{ICF}$, lysosomes, brain phospholipids, lateral ventricles, third and fourth ventricles, cisterna magna, and subarachnoid space. Model parameters were changed by 10% and 200%, while pH values were altered by 0.1 and 2 pH units. The C_{max}, T_{max}, AUC, and half-life of the PK profiles from the healthy and altered CNS parameters were then compared.

3. Results

The predicted PK profiles of plasma and $brain_{ECF}$ of Remdesivir, GS441524, Nirmatrelvir, and EIDD1931 are presented in figure 1. The predicted $brain_{ECF}$ PK profiles are depicted against the in vitro EC_{90} values specific for the delta and omicron variants, except for GS441524 which is depicted against the EC_{50} value, as the EC_{90} values specific for the delta and omicron variants were not available. Extracellular PK profiles were compared against the EC_{90} values, since the in vitro EC_{90} values reflect extracellular and not intracellular drug concentrations.

The predicted $brain_{ECF}$ PK profile of Nirmatrelvir was consistently above the EC_{90} value of both variants, with an average efficacy of 87% and 96% against the delta and omicron variants, respectively. Nirmatrelvir still achieved effective $brain_{ECF}$ PK profiles following a 50% reduction of plasma C_{max} (supplementary figure 1, online resource 1). The reduction of plasma C_{max} was achieved with an 85% lower absorption rate constant to account for the formulation differences between tablets and oral suspensions (European Medicines Agency, 2021b). The predicted $brain_{ECF}$ PK profiles of Remdesivir and of GS441524 were below the EC_{90}. The predicted $brain_{ICF}$ PK profile of GS443902 against the intracellular EC_{90} value are described in figure 2. The intracellular EC_{90} value was calculated based on the extracellular EC_{90} value of Remdesivir and the average intracellular levels of GS443902 (Pruijssers et al., 2020). $Brain_{ICF}$ concentrations profile of GS443902 increased over time with each dose, but remained, however, below the intracellular EC_{90}.

The predicted $brain_{ECF}$ PK of EIDD1931 was below the EC_{90} of the two variants. EIDD2061 $brain_{ICF}$ PK profile, reported in figure 2, does not notably accumulate continuously in brain (Painter et al., 2019), mainly because of its short half-life. Data required to calculate the intracellular $EC_{50/90}$ of EIDD2061 were not available. The average concentration ratio of EIDD2061 to EIDD1931 is between one-third and two, as measured in mice spleen and brain, respectively (Painter et al., 2019). This means that the intracellular EC_{90} of EIDD2061 can be assumed to be (at best) threefold lower than that measured extracellularly for EIDD1931 or 1.55 nmol/ml, which is still three times higher than the predicted intracellular C_{max} of EIDD2061 (0.4 nmol/ml).

In this study, LeiCNS-PK3.0 simulations were performed using the parameters of the healthy human CNS. Therefore, a sensitivity analysis was performed to assess the PK changes caused by the potential COVID-19 alterations of CNS physiology. Changes of pH_{ECF} and pH_{ICF} resulted in the largest change of $brain_{ECF}$ and $brain_{ICF}$ PK of Nirmatrelvir (pKa = 7.1, table 1). Remdesivir and EIDD1931 are neutral molecules and thus not impacted by pH changes. Also, changes of brain cell volume and surface area impacted the PK of EIDD1931.

4. Discussion

The neurotrophic characteristics and the associated neurological manifestations of SARS-CoV-2 strongly imply the need to eradicate the virus from the brain. CNS penetration of small molecules approved for COVID-19 have not been studied in humans. Using the LeiCNS-PK3.0 PBPK framework and the recommended dosing regimen, we predict that Nirmatrelvir alone achieves adequate PK profiles as based on in vitro EC_{90} values against SARS-CoV-2 variants of interest, i.e. the delta and omicron variants. These results can guide clinical trials on the assessment of efficacy of antiCOVID-19 drugs in the human CNS.

Based on our model simulations, the dose of Remdesivir or Molnupiravir required to achieve effective concentrations in the brain cells will exceed by several folds the highest dose that was tested during the clinical development of both drugs. A minimum dose of 300 mg twice daily of Remdesivir was needed for the $brain_{ICF}$ C_{min} of GS443902 to be higher than the calculated intracellular EC_{90} value (1.78 pmol/million cell (Pruijssers et al., 2020)). With regards to Molnupiravir, a dose of 4000 mg twice daily was required for the intracellular C_{min} of EIDD2061 to exceed the lowest predicted intracellular EC_{90} value of 1.55 nmol/ml. Both doses were not explored in the dose escalation studies in humans (Humeniuk et al., 2020; Painter et al., 2021) and thus the associated potential toxicities have not been investigated.

COVID-19 is associated with distinct CNS pathophysiological alterations. SARS-CoV-2 impaired the integrity of the BBB, either because of the impairment of the basement membrane without affecting tight junctions (Krasemann et al., 2022; Zhang et al., 2021) or the loss of tight junction proteins (Buzhdygan et al., 2020; Erickson et al., 2021; Reynolds and Mahajan, 2021; Wang et al., 2021). Also, the increased protein content in CSF (Jarius et al., 2022; Tandon et al., 2021) suggests a breakdown of the BCSFB (Pellegrini et al., 2020), but could also be a result of decreased CSF flow (Reiber, 1994). SARS-CoV-2 infection might result in brain atrophy, wherein the volume of gray matter significantly reduced than white matter (Douaud et al., 2022; Qin et al., 2021). No direct evidence suggests the changes in the volume and the surface area of brain cells. Many COVID-19 patients, however, present with hypoxemia (Dhont et al., 2020; Solomon et al., 2020), which in turn, results in the increase of anaerobic metabolism in the mitochondria of brain cells (Abdennour et al., 2012). The accumulation of lactic acid produced by mitochondria can cause swelling of brain cells (Duan et al., 2021; Juzekaeva et al., 2018). In addition, patients recovered from severe COVID-19 have significantly reduced cortical cerebral blood flow (Qin et al., 2021). While no reports on the impact of SARS-CoV-2 on $brain_{ECF}$ pH, the accumulation of lactic acid due to anerobic respiration might results in a lower brain pH (Fan et al., 2020). In addition, influenza virus results in a decreased $brain_{ECF}$ pH, by H+ export from cells (Liu et al., 2016). Hence, we performed a sensitivity analysis to study the impact of these pathophysiological changes on brain PK with a focus on C_{max} and exposure given by the AUC (Supplementary figure 2, online resource 1). An increase of brain cell volume as a result of brain cell swelling will reduce the C_{max} and AUC of EIDD1931. A decrease of pH_{ECF} slightly decreased the C_{max} of $brain_{ECF}$ and increased the C_{max} and exposure of $brain_{ICF}$. Therefore, based on the sensitivity analysis results and the literature summary of CNS pathophysiology in COVID-19, small changes (10%) of CNS physiology as expected in COVID-19 will not notably impact the brain PK profiles. We therefore postulate that our simulation results using healthy CNS parameters still apply for COVID-19 patients, independent of the disease state of the CNS.

In this simulation study, asymmetry factors (AF), which represent active transport activity at BBB, were calculated based on $Kp_{uu,BBB}$ values provided by “the brain exposure efficiency” (BEE) in silico calculator (Gupta et al., 2020) for Nirmatrelvir and Remdesivir, both drugs being P-glycoprotein substrates. The predicted $Kp_{uu,BBB}$ of Remdesivir was in line with total brain-to-plasma Remdesivir ratios measured in radiographic imaging studies in rats (Gilead Sciences, 2020) and in rhesus monkeys (Warren et al., 2016). No in vivo or in vitro data on P-glycoprotein activity were available for Nirmatrelvir. To assess the impact of the uncertainty associated with the predicted $Kp_{uu,BBB}$ (and consequently AF) on brain PK, we explored the scenario assuming a five-fold increase of BBB p-glycoprotein activity (i.e. a five-fold decrease of $Kp_{uu,BBB}$), Nirmatrelvir still maintained activity against the omicron, but not the delta, variant (results not shown). Future in vitro or preclinical in vivo studies addressing the brain penetration of Nirmatrelvir are required to further substantiate these outcomes.

Remdesivir and Molnupiravir are prodrugs of the parent nucleosides and undergo intracellular metabolism to the active nucleoside analogues, GS443902 and EIDD2061, respectively. $EC_{50/90}$ were derived from in vitro systems that were based on animal and human cell lines and vary by the metabolic capacity of these cell lines depending on the enzyme expression. Protein expression of human brain kinase and HINT1/3 (phosphoramidase enzymes) were comparable or lower to those of human lungs and liver (Sjöstedt et al., 2020), maintaining our earlier conclusion.

5. Conclusion

With the LeiCNS-PK3.0 PBPK framework, we predict that with the current dosing regimen only Nirmatrelvir and not Remdesivir or Molnupiravir will reach effective PK against the delta and the omicron variants in the human brain. Our study provides evidence-based guidance for the design of future (pre)clinical studies addressing the antiCOVID-19 drug efficacy in the human CNS.

6. Author Contributions

Mohammed AA Saleh, Jeroen Elassaiss-Schaap, Elizabeth CM de Lange contributed to project conceptualization, Mohammed AA Saleh, Ming Sun, and Berfin Gülave performed the data collection, Mohammed AA Saleh and Makoto Hirasawa performed the data analysis and model simulations, Mohammed AA Saleh, Jeroen Elassaiss-Schaap and Elizabeth CM de Lange drafted and reviewed the manuscript.

Supplementary materials: Supplementary figures 1 and 2 are included in electronic supplementary materials ESM_1.pdf

Funding

This research was funded by Leiden Academic Center for Drug Research (LACDR), Leiden University, Leiden, The Netherlands.

Declaration of Competing Interest

Makoto Hirasawa is an employee of Daiichi-Sankyo Co., Ltd.

References

Abdennour, L., Zeghal, C., Dème, M., Puybasset, L., 2012. Interaction cerveau-poumon. Ann. Fr. Anesth. Reanim. 31, 101–107. https://doi.org/10.1016/j.annfar.2012.04.013

Buzhdygan, T.P., DeOre, B.J., Baldwin-Leclair, A., Bullock, T.A., McGary, H.M., Khan, J.A., Razmpour, R., Hale, J.F., Galie, P.A., Potula, R., Andrews, A.M., Ramirez, S.H., 2020. The SARS-CoV-2 spike protein alters barrier function in 2D static and 3D microfluidic in-vitro models of the human blood–brain barrier.

Neurobiol. Dis. 146, 105131. https://doi.org/10.1016/j.nbd.2020.105131

Chou, S.H.Y., Beghi, E., Helbok, R., Moro, E., Sampson, J., Altamirano, V., Mainali, S., Bassetti, C., Suarez, J.I., McNett, M., 2021. Global Incidence of Neurological Manifestations among Patients Hospitalized with COVID-19 - A Report for the GCS-NeuroCOVID Consortium and the ENERGY Consortium. JAMA Netw. Open 4, 1–14. https://doi.org/10.1001/jamanetworkopen.2021.12131

Coordinators, N.R., 2018. Database resources of the National Center for Biotechnology Information. Nucleic Acids Res. 46, D8–D13. https://doi.org/10.1093/nar/gkx1095

Dhont, S., Derom, E., Van Braeckel, E., Depuydt, P., Lambrecht, B.N., 2020. The pathophysiology of 'happy' hypoxemia in COVID-19. Respir. Res. 21, 1–9. https://doi.org/10.1186/s12931-021-01614-1

Douaud, G., Lee, S., Alfaro-Almagro, F., Arthofer, C., Wang, C., McCarthy, P., Lange, F., Andersson, J.L.R., Griffanti, L., Duff, E., Jbabdi, S., Taschler, B., Keating, P., Winkler, A.M., Collins, R., Matthews, P.M., Allen, N., Miller, K.L., Nichols, T.E., Smith, S.M., 2022. SARS-CoV-2 is associated with changes in brain structure in UK Biobank. Nature 604, 697–707. https://doi.org/10.1038/s41586-022-04569-5

Duan, K., Premi, E., Pilotto, A., Cristillo, V., Benussi, A., Libri, I., Giunta, M., Bockholt, H.J., Liu, J., Campora, R., Pezzini, A., Gasparotti, R., Magoni, M., Padovani, A., Calhoun, V.D., 2021. Alterations of frontal-temporal gray matter volume associate with clinical measures of older adults with COVID-19. Neurobiol. Stress 14. https://doi.org/10.1016/j.ynstr.2021.100326

Erickson, M.A., Rhea, E.M., Knopp, R.C., 2021. Interactions of SARS-CoV-2 with the Blood – Brain Barrier. Int. J. Mol. Sci. 22, 1–28. https://doi.org/10.3390/ijms22052681

European Medicines Agency, 2021a. Assessment report on the Use of molnupiravir for the treatment of COVID-19 [WWW Document]. Eur. Med. Agency. URL https://www.ema.europa.eu/en/documents/referral/lagevrio-also-known-molnupiravir-mk-4482-covid-19-article-53-procedure-assessment-report_en.pdf (accessed 2.1.22).

European Medicines Agency, 2021b. Assessment report on paxlovid use in COVID-19 [WWW Document]. Eur. Med. Agency. URL https://www.ema.europa.eu/en/documents/referral/paxlovid-pf-07321332-ritonavir-covid-19-article-53-procedure-assessment-report_en.pdf (accessed 2.1.22).

European Medicines Agency, 2020. Assessment report on the use of Veklury in the treatment of COVID-19

[WWW Document]. Eur. Med. Agency. URL https://www.ema.europa.eu/en/documents/assessment-report/veklury-epar-public-assessment-report_en.pdf (accessed 2.1.22).

Fan, H., Tang, X., Song, Y., Liu, P., Chen, Y., 2020. Influence of covid-19 on cerebrovascular disease and its possible mechanism. Neuropsychiatr. Dis. Treat. 16, 1359–1367. https://doi.org/10.2147/NDT.S251173

Fidler, M., Hallow, M., Wilkins, J., Wang, W., 2019. RxODE: Facilities for Simulating from ODE-Based Models.

Gilead Sciences, 2020. Pharmacokinetics written summary (Remdesivir) [WWW Document]. Prod. Doc. URL https://www.pmda.go.jp/drugs/2020/P20200518003/230867000_30200AMX00455_I100_1.pdf (accessed 2.1.22).

Gonçalves, A., Bertrand, J., Ke, R., Comets, E., de Lamballerie, X., Malvy, D., Pizzorno, A., Terrier, O., Rosa Calatrava, M., Mentré, F., Smith, P., Perelson, A.S., Guedj, J., 2020. Timing of Antiviral Treatment Initiation is Critical to Reduce SARS-CoV-2 Viral Load. CPT Pharmacometrics Syst. Pharmacol. 9, 509–514. https://doi.org/10.1002/psp4.12543

Guadarrama-Ortiz, P., Choreño-Parra, J.A., Sánchez-Martínez, C.M., Pacheco-Sánchez, F.J., Rodríguez-Nava, A.I., García-Quintero, G., 2020. Neurological Aspects of SARS-CoV-2 Infection: Mechanisms and Manifestations. Front. Neurol. 11, 1–14. https://doi.org/10.3389/fneur.2020.01039

Gupta, M., Bogdanowicz, T., Reed, M.A., Barden, C.J., Weaver, D.F., 2020. The Brain Exposure Efficiency (BEE) Score. ACS Chem. Neurosci. 11, 205–224. https://doi.org/10.1021/acschemneuro.9b00650

Humeniuk, R., Mathias, A., Cao, H., Osinusi, A., Shen, G., Chng, E., Ling, J., Vu, A., German, P., 2020. Safety, Tolerability, and Pharmacokinetics of Remdesivir, An Antiviral for Treatment of COVID-19, in Healthy Subjects. Clin. Transl. Sci. 13, 896–906. https://doi.org/10.1111/cts.12840

Humeniuk, R., Mathias, A., Kirby, B.J., Lutz, J.D., Cao, H., Osinusi, A., Babusis, D., Porter, D., Wei, X., Ling, J., Reddy, Y.S., German, P., 2021. Pharmacokinetic, Pharmacodynamic, and Drug-Interaction Profile of Remdesivir, a SARS-CoV-2 Replication Inhibitor. Clin. Pharmacokinet. 60, 569–583. https://doi.org/10.1007/s40262-021-00984-5

Jarius, S., Pache, F., Körtvelyessy, P., Jelčić, I., Stettner, M., Franciotta, D., Keller, E., Neumann, B., Ringelstein, M., Senel, M., Regeniter, A., Kalantzis, R., Willms, J.F., Berthele, A., Busch, M., Capobianco, M., Eisele, A., Reichen, I., Dersch, R., Rauer, S., Sandner, K., Ayzenberg, I., Gross, C.C., Hegen, H., Khalil, M., Kleiter, I., Lenhard, T., Haas, J., Aktas, O., Angstwurm, K., Kleinschnitz, C., Lewerenz, J., Tumani, H., Paul, F., Stangel, M., Ruprecht, K., Wildemann, B., 2022. Cerebrospinal fluid findings in COVID-19: a multicenter study of 150 lumbar punctures in 127 patients. J. Neuroinflammation 19, 1–33. https://doi.org/10.1186/s12974-021-02339-0

Juzekaeva, E., Gainutdinov, A., Mukhtarov, M., Khazipov, R., 2018. Dynamics of the hypoxia—induced tissue edema in the rat barrel cortex in vitro. Front. Cell. Neurosci. 12, 1–11. https://doi.org/10.3389/fncel.2018.00502

Krasemann, S., Haferkamp, U., Pfefferle, S., Woo, M.S., Heinrich, F., Schweizer, M., Appelt-Menzel, A., Cubukova, A., Barenberg, J., Leu, J., Hartmann, K., Thies, E., Littau, J.L., Sepulveda-Falla, D., Zhang, L., Ton, K., Liang, Y., Matschke, J., Ricklefs, F., Sauvigny, T., Sperhake, J., Fitzek, A., Gerhartl, A., Brachner, A., Geiger, N., König, E.M., Bodem, J., Franzenburg, S., Franke, A., Moese, S., Müller, F.J., Geisslinger, G., Claussen, C., Kannt, A., Zaliani, A., Gribbon, P., Ondruschka, B., Neuhaus, W., Friese, M.A., Glatzel, M., Pless, O., 2022. The blood-brain barrier is dysregulated in COVID-19 and serves as a CNS entry route for SARS-CoV-2. Stem Cell Reports 17, 307–320. https://doi.org/10.1016/j.stemcr.2021.12.011

Liu, H., Maruyama, H., Masuda, T., Honda, A., Arai, F., 2016. The influence of virus infection on the extracellular pH of the host cell detected on cell membrane. Front. Microbiol. 7, 1–8. https://doi.org/10.3389/fmicb.2016.01127

Matschke, J., Lütgehetmann, M., Hagel, C., Sperhake, J.P., Schröder, A.S., Edler, C., Mushumba, H., Fitzek, A., Allweiss, L., Dandri, M., Dottermusch, M., Heinemann, A., Pfefferle, S., Schwabenland, M., Sumner Magruder, D., Bonn, S., Prinz, M., Gerloff, C., Püschel, K., Krasemann, S., Aepfelbacher, M., Glatzel, M., 2020. Neuropathology of patients with COVID-19 in Germany: a post-mortem case series. Lancet Neurol. 19, 919–929. https://doi.org/10.1016/S1474-4422(20)30308-2

Pacheco-Herrero, M., Soto-Rojas, L.O., Harrington, C.R., Flores-Martinez, Y.M., Villegas-Rojas, M.M., León-Aguilar, A.M., Martínez-Gómez, P.A., Campa-Córdoba, B.B., Apátiga-Pérez, R., Corniel-Taveras, C.N., Dominguez-García, J. de J., Blanco-Alvarez, V.M., Luna-Muñoz, J., 2021. Elucidating the Neuropathologic Mechanisms of SARS-CoV-2 Infection. Front. Neurol. 12, 1–19. https://doi.org/10.3389/fneur.2021.660087

Painter, G.R., Bowen, R.A., Bluemling, G.R., DeBergh, J., Edpuganti, V., Gruddanti, P.R., Guthrie, D.B., Hager, M., Kuiper, D.L., Lockwood, M.A., Mitchell, D.G., Natchus, M.G., Sticher, Z.M., Kolykhalov, A.A., 2019. The prophylactic and therapeutic activity of a broadly active ribonucleoside analog in a murine model of intranasal venezuelan equine encephalitis virus infection. Antiviral Res. 171, 1–10. https://doi.org/10.1016/j.antiviral.2019.104597

Painter, W.P., Holman, W., Bush, J.A., Almazedi, F., Malik, H., Eraut, N.C.J.E., Morin, M.J., Szewczyk, L.J., Painter, G.R., 2021. Human safety, tolerability, and pharmacokinetics of molnupiravir, a novel broad-spectrum oral antiviral agent with activity against SARS-CoV-2. Antimicrob. Agents Chemother. 65. https://doi.org/10.1128/AAC.02428-20

Pellegrini, L., Albecka, A., Mallery, D.L., Kellner, M.J., Paul, D., Carter, A.P., James, L.C., Lancaster, M.A., 2020. SARS-CoV-2 Infects the Brain Choroid Plexus and Disrupts the Blood-CSF Barrier in Human Brain Organoids. Cell Stem Cell 27, 951-961.e5. https://doi.org/10.1016/j.stem.2020.10.001

Philippens, I.H.C.H.M., Böszörményi, K.P., Wubben, J.A., Fagrouch, Z.C., Driel, N. van, Mayenburg, A.Q., Lozovagia, D., Roos, E., Schurink, B., Bugiani, M., Bontrop, R.E., Middeldorp, J., Bogers, W.M., Geus-Oei, L.-F. de, Langermans, J.A.M., Stammes, M.A., Verstrepen, B.E., Verschoor, E.J., 2021. SARS-CoV-2 causes brain inflammation and induces Lewy body formation in macaques. BIORXIV. https://doi.org/10.1101/2021.02.23.432474

Pruijssers, A.J., George, A.S., Schäfer, A., Leist, S.R., Gralinksi, L.E., Dinnon, K.H., Yount, B.L., Agostini, M.L., Stevens, L.J., Chappell, J.D., Lu, X., Hughes, T.M., Gully, K., Martinez, D.R., Brown, A.J., Graham, R.L., Perry, J.K., Du Pont, V., Pitts, J., Ma, B., Babusis, D., Murakami, E., Feng, J.Y., Bilello, J.P., Porter, D.P., Cihlar, T., Baric, R.S., Denison, M.R., Sheahan, T.P., 2020. Remdesivir Inhibits SARS-CoV-2 in Human Lung Cells and Chimeric SARS-CoV Expressing the SARS-CoV-2 RNA Polymerase in Mice. Cell Rep. 32. https://doi.org/10.1016/j.celrep.2020.107940

Qin, Y., Wu, J., Chen, T., Li, J., Zhang, G., Wu, D., Zhou, Y., Zheng, N., Cai, A., Ning, Q., Manyande, A., Xu, F., Wang, J., Zhu, W., 2021. Long-term microstructure and cerebral blood flow changes in patients recovered from COVID-19 without neurological manifestations. J. Clin. Invest. 131, 1–12. https://doi.org/10.1172/JCI147329

R Core Team, 2019. R: A language and environment for statistical computing. R Foundation for Statistical

Computing, Vienna, Austria.

Reiber, H., 1994. Flow rate of cerebrospinal fluid (CSF) - A concept common to normal blood-CSF barrier function and to dysfunction in neurological diseases. J. Neurol. Sci. 122, 189–203. https://doi.org/10.1016/0022-510X(94)90298-4

Reynolds, J.L., Mahajan, S.D., 2021. SARS-COV2 Alters Blood Brain Barrier Integrity Contributing to Neuro-Inflammation. J. Neuroimmune Pharmacol. 16, 4–6. https://doi.org/10.1007/s11481-020-09975-y

Rosales, R., Rodriguez, M.L., Rai, D.K., Cardin, R.D., Anderson, A.S., Sordillo, E.M., Bakel, H. van, Simon, V., García-Sastre, A., White, K.M., 2022. Nirmatrelvir, Molnupiravir, and Remdesivir maintain potent in vitro activity against the SARS-CoV-2 Omicron variant. bioRxiv 2019.

Saleh, M.A.A., de Lange, E.C.M., 2021. Impact of CNS Diseases on Drug Delivery to Brain Extracellular and Intracellular Target Sites in Human: A "WHAT-IF" Simulation Study. Pharmaceutics 13, 1–17. https://doi.org/10.3390/pharmaceutics13010095

Saleh, M.A.A., Loo, C.F., Elassaiss-Schaap, J., De Lange, E.C.M., 2021. Lumbar cerebrospinal fluid-to-brain extracellular fluid surrogacy is context-specific: insights from LeiCNS-PK3.0 simulations. J. Pharmacokinet. Pharmacodyn. 48, 725–741. https://doi.org/10.1007/s10928-021-09768-7

Shen, W., Logue, J., Yang, Penghua, Baracco, L., Elahi, M., Reece, A., Wang, B., Li, L., Blanchard, T.G., Han, Z., Frieman, M.B., Rissman, R.A., Yang, Peixin, 2022. SARS-CoV-2 invades cognitive centers of the brain and induces Alzheimer's-like neuropathology. Bior. https://doi.org/10.1101/2022.01.31.478476

Sjöstedt, E., Zhong, W., Fagerberg, L., Karlsson, M., Mitsios, N., Adori, C., Oksvold, P., Edfors, F., Limiszewska, A., Hikmet, F., Huang, J., Du, Y., Lin, L., Dong, Z., Yang, L., Liu, X., Jiang, H., Xu, X., Wang, J., Yang, H., Bolund, L., Mardinoglu, A., Zhang, C., Feilitzen, K. von, Lindskog, C., Pontén, F., Luo, Y., Hökfelt, T., Uhlén, M., Mulder, J., 2020. An atlas of the protein-coding genes in the human, pig, and mouse brain. Science (80-.). 367, eaay5947. https://doi.org/10.1126/science.aay5947

Solomon, I.H., Normandin, E., Bhattacharyya, S., Mukerji, S.S., Kiana Keller, Ali, A.S., Adams, G., Hornick, J.L., Padera, R.F., Sabeti, P., 2020. Neuropathological Features of Covid-19. N. Engl. J. Med. 383, 986–989. https://doi.org/10.1056/nejmc2001362

Stein, S., Ramelli, S., Grazioli, A., Winkler, C., Dickey, J., Platt, A., Pittaluga, S., Herr, D., Mccurdy, M., Consortium, N.C.-19 A., Peterson, K.E., Cohen, J.I., Wit, E. de, Vannella, K.M., Hewitt, S.M., Kleiner, D.E., Chertow, D.S., 2021. SARS-CoV-2 infection and persistence throughout the human body and brain. Res. Sq. https://doi.org/10.21203/rs.3.rs-1139035/v1

Tandon, M., Kataria, S., Patel, J., Mehta, T.R., Daimee, M., Patel, V., Prasad, A., Chowdhary, A.A., Jaiswal, S., Sriwastava, S., 2021. A Comprehensive Systematic Review of CSF analysis that defines Neurological Manifestations of COVID-19. Int. J. Infect. Dis. 104, 390–397. https://doi.org/10.1016/j.ijid.2021.01.002

Tao, S., Zandi, K., Bassit, L., Ong, Y.T., Verma, K., Liu, P., Downs-Bowen, J.A., McBrayer, T., LeCher, J.C., Kohler, J.J., Tedbury, P.R., Kim, B., Amblard, F., Sarafianos, S.G., Schinazi, R.F., 2021. Comparison of anti-SARS-CoV-2 activity and intracellular metabolism of remdesivir and its parent nucleoside. Curr. Res. Pharmacol. Drug Discov. 2, 100045. https://doi.org/10.1016/j.crphar.2021.100045

U.S. Food and Drug Administration, 2020. Clinical Pharmacology and Biopharmaceutics Review (Remdesivir) [WWW Document]. U.S. Food Drug Adm. URL https://www.accessdata.fda.gov/drugsatfda_docs/nda/2020/214787Orig1s000ClinpharmR.pdf

Vangeel, L., Chiu, W., De Jonghe, S., Maes, P., Slechten, B., Raymenants, J., André, E., Leyssen, P., Neyts, J., Jochmans, D., 2022. Remdesivir, Molnupiravir and Nirmatrelvir remain active against SARS-CoV-2 Omicron and other variants of concern. Antiviral Res. 198, 105252. https://doi.org/10.1016/j.antiviral.2022.105252

Veleri, S., 2022. Neurotropism of SARS-CoV-2 and neurological diseases of the central nervous system in COVID-19 patients. Exp. Brain Res. 240, 9–25. https://doi.org/10.1007/s00221-021-06244-z

Wang, P., Jin, L., Zhang, M., Wu, Y., Duan, Z., Chen, W., Wang, C., Liao, Z., Han, J., Guo, Yingqi, Guo, Yaqiong, Wang, Y., Lai, R., Qin, J., 2021. SARS-CoV-2 causes human BBB injury and neuroinflammation indirectly in a linked organ chip platform. bioRxiv.

Warren, T.K., Jordan, R., Lo, M.K., Ray, A.S., Mackman, R.L., Soloveva, V., Siegel, D., Perron, M., Bannister, R., Hui, H.C., Larson, N., Strickley, R., Wells, J., Stuthman, K.S., Van Tongeren, S.A., Garza, N.L., Donnelly, G., Shurtleff, A.C., Retterer, C.J., Gharaibeh, D., Zamani, R., Kenny, T., Eaton, B.P., Grimes, E., Welch, L.S., Gomba, L., Wilhelmsen, C.L., Nichols, D.K., Nuss, J.E., Nagle, E.R., Kugelman, J.R., Palacios, G., Doerffler, E., Neville, S., Carra, E., Clarke, M.O., Zhang, L., Lew, W., Ross, B., Wang, Q., Chun, K., Wolfe, L., Babusis, D., Park, Y., Stray, K.M., Trancheva, I., Feng, J.Y., Barauskas, O., Xu, Y., Wong, P., Braun, M.R., Flint, M., McMullan, L.K., Chen, S.S., Fearns, R., Swaminathan, S., Mayers, D.L., Spiropoulou, C.F., Lee, W.A., Nichol, S.T., Cihlar, T., Bavari, S., 2016. Therapeutic efficacy of the small molecule GS-5734 against Ebola virus in rhesus monkeys. Nature 531, 381–385. https://doi.org/10.1038/nature17180

Wishart, D.S., Feunang, Y.D., Guo, A.C., Lo, E.J., Marcu, A., Grant, J.R., Sajed, T., Johnson, D., Li, C., Sayeeda, Z., Iynkkaran, N.A.I., Liu, Y., Maciejewski, A., Gale, N., AlexWilson, Chin, L., Cummings, R., Le, D., Pon, A., Knox, C., Wilson, M., 2017. DrugBank 5.0: a major update to the DrugBank database for 2018. Nucleic Acids Res. 46, D1074–D1082. https://doi.org/10.1093/nar/gkx1037

World Health Organization (WHO), n.d. Tracking SARS-CoV-2 variants [WWW Document]. URL https://www.who.int/en/activities/tracking-SARS-CoV-2-variants/ (accessed 4.6.22).

Yang, A.C., Kern, F., Losada, P.M., Agam, M.R., Maat, C.A., Schmartz, G.P., Fehlmann, T., Stein, J.A., Schaum, N., Lee, D.P., Calcuttawala, K., Vest, R.T., Berdnik, D., Lu, N., Hahn, O., Gate, D., McNerney, M.W., Channappa, D., Cobos, I., Ludwig, N., Schulz-Schaeffer, W.J., Keller, A., Wyss-Coray, T., 2021. Dysregulation of brain and choroid plexus cell types in severe COVID-19. Nature 595, 565–571. https://doi.org/10.1038/s41586-021-03710-0

Zhang, L., Zhou, L., Bao, L., Liu, J., Zhu, H., Lv, Q., Liu, R., Chen, W., Tong, W., Wei, Q., Xu, Y., Deng, W., Gao, H., Xue, J., Song, Z., Yu, P., Han, Y., Zhang, Y., Sun, X., Yu, X., Qin, C., 2021. SARS-CoV-2 crosses the blood–brain barrier accompanied with basement membrane disruption without tight junctions alteration. Signal Transduct. Target. Ther. 6. https://doi.org/10.1038/s41392-021-00719-9

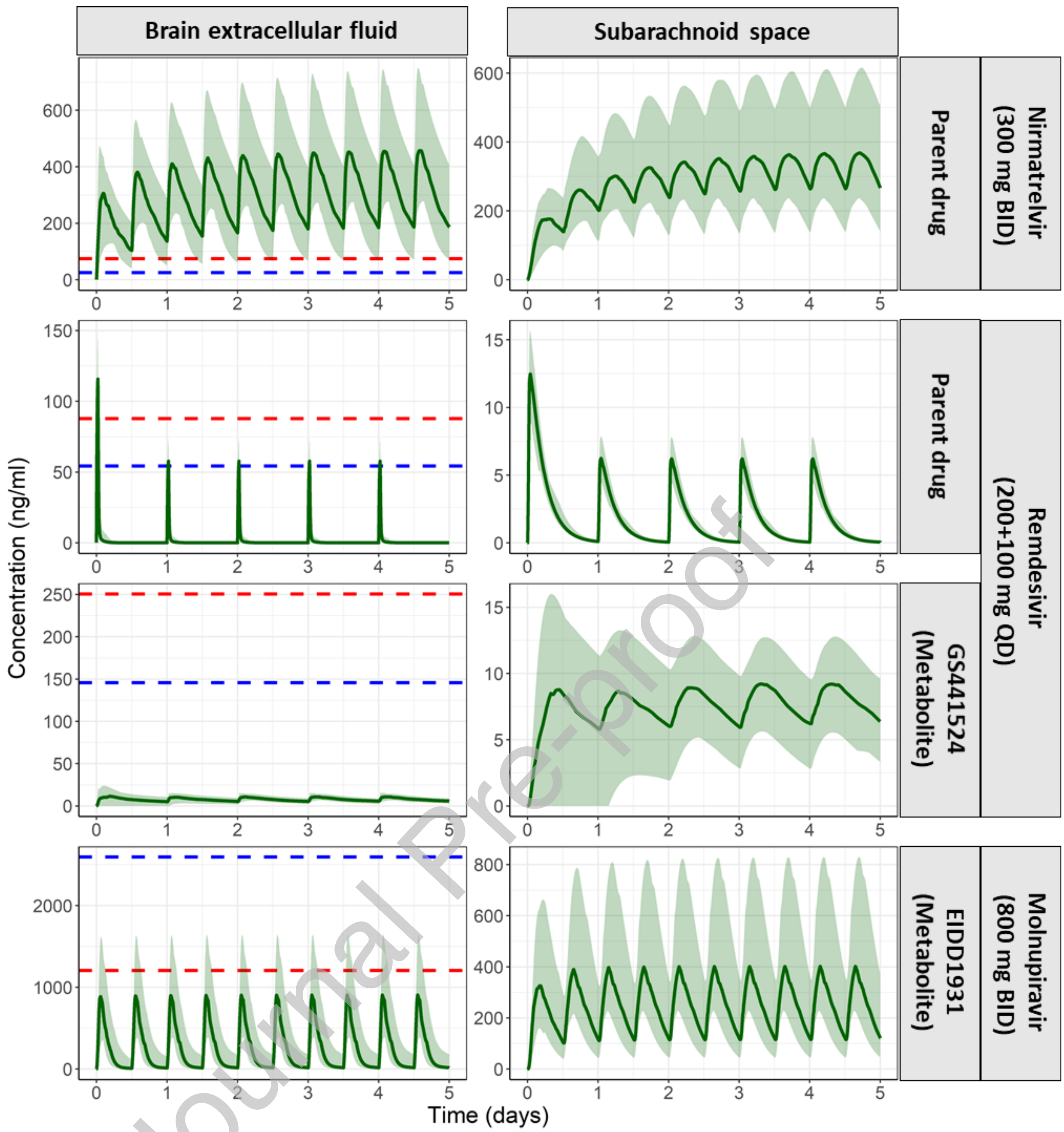

Fig. 1 CNS PK predictions of LeiCNS-PK3.0 of drugs approved for COVID-19 treatment. Median (solid green line) and 95 percentiles (green shaded area) of brain$_{ECF}$ and subarachnoid space PK profiles of Nirmatrelvir, EIDD1931 (Molnupiravir plasma metabolite), and Remdesivir, in addition to Remdesivir metabolite, GS441524. The PK profiles are depicted against the EC_{90} (dashed lines) against the omicron (blue) and the delta (red) variants. The concentrations of Nirmatrelvir only were above the respective EC_{90} of both variants, with an average efficacy of 87% and 96% against the delta and omicron variants, respectively.

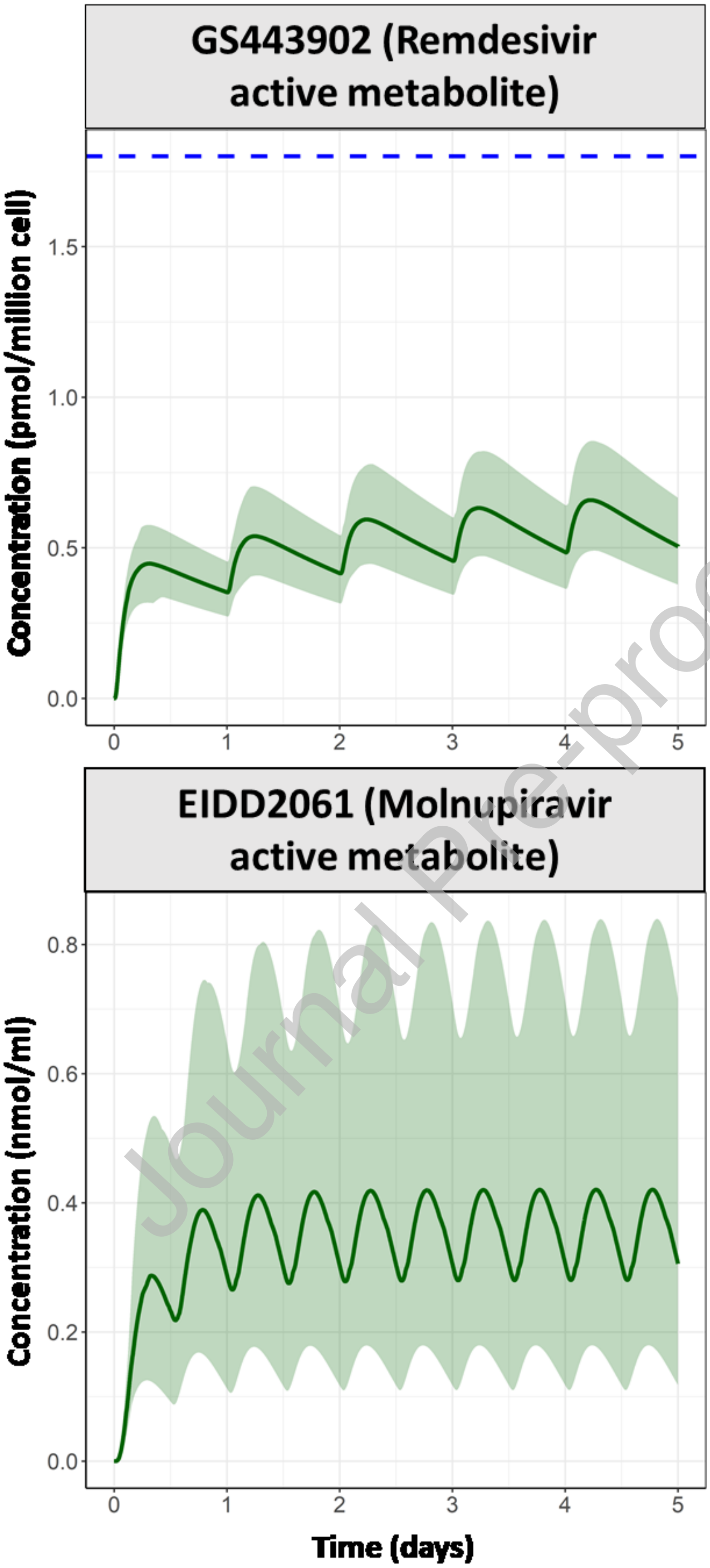
GS443902 (Remdesivir active metabolite)
EIDD2061 (Molnupiravir active metabolite)
Concentration (pmol/million cell)
Concentration (nmol/ml)
1.5
1.0
0.5
0.0
0.8
0.6
0.4
0.2
0.0
0
1
2
3
4
5
Time (days)

Fig. 2 Median (solid green line) and 95 percentiles (green shaded area) of the predicted intracellular levels of GS443902 (top) and EIDD2061 (bottom), the active triphosphate metabolites of Molnupiravir and Remdesivir, respectively. GS443902 is hydrophilic (logP = -5.3 (Coordinators, 2018)), with an elimination half-life of 43.4 hours (Humeniuk et al., 2021), which indicate its potential for intracellular accumulation. At the recommended dosing, however, GS443902 predicted levels are below the intracellular EC_{90} value (1.78 pmol/million cell (Pruijssers et al., 2020), dashed blue line) against USA-WA1/2020. EIDD2061 is also hydrophilic, but with a relatively short half-life of 4.5 hr (European Medicines Agency, 2021a) and therefore does not accumulate extensively intracellularly (Painter et al., 2019). Data required for calculating intracellular EC_{90} of EIDD2061 were not available. EIDD2061 intracellular predicted C_{max} is however ten fold lower than the EC_{90} reported for EIDD1931, while the average concentration ratio of EIDD2061 to EIDD1931 ranges from one-third to two. Thus, intracellular EC_{90} can be as low as 1.55 nmol/ml, which is still three times the C_{max} of EIDD2061 at the recommended dosing regimen

Table 1. LeiCNS-PK3.0 input parameters

Drug	Nirmatrelvir	Remdesivir			Molnupiravir
	Parent	Parent	Metabolites		Metabolite
			GS704277	GS441524	EIDD1931
Physicochemical properties (Wishart et al., 2017)					
MW (g/mol)	499.535	602.585	442.32	291.267	259.218
LogP (unitless)	2.12	2.01	-0.88	-0.58	-2
pK_a (unitless)	7.1	10.23	2.38	12.13	12.55
pK_b (unitless)	-1.6	0.65	0.64	0.65	2.39
Plasma PK (European Medicines Agency, 2021a, 2021b; U.S. Food and Drug Administration, 2020)					
CL_{cen} (mL min^{-1})	17	803.33	3500	2933.33	1281.667
$Q_{cen-per1}$ (mL min^{-1})	7.4	84	341.667	6316.667	55.833
$Q_{cen-per2}$ (mL min^{-1})	0	0	0	526.667	0
V_{cen} (mL)	8200	6340	242000	104000	72000
V_{per1} (mL)	5650	6000	46000	236000	70000
V_{per2} (mL)	0	0	0	233000	0

Ka (min^{-1})	0.3783	not applicable	not applicable	not applicable	0.01383
D1 (min)	NA	not applicable	not applicable	not applicable	48.12
IIV on CL_{cen}	0.264	0.387	0.565	0.4898	0.411
IIV on $Q_{cen\text{-}per1}$	0	0	0	0	0
IIV on $Q_{cen\text{-}per2}$	0	0.5656	0	0	0
IIV on V_{cen}	0.307	0.387	0.6244	0.67	0.4
IIV on V_{per1}	0.699	0.5656	0.5099	0.6557	0
IIV on V_{per2}	0	0	0	0.5	0
IIV on Ka	0.576	NA	NA	NA	0
IIV on D1	0	NA	NA	NA	0.428
Proportional residual error	0.0336	0.45	0.44	0.31	0.442
Additive residual error (ng/ml)	399	0.884	0.604	0.511	0
Drug biological parameters					
fu,p	0.31	0.121	0.98	0.99	1
$Kp_{uu,BBB}$	0.35[a]	0.14[a]	0.07[a]	0.22[a]	0.4[b]
$AF_{ef,BBB}$	3.02	7.97	23864402	696.67	1719.71
$Kp_{uu,LV}$	0.35[c]	0.14[c]	0.07[c]	0.22[c]	0.4[c]
$AF_{ef,LV}$	4.67	10.46	94737456	2739.28	6773.89
$Kp_{uu,SAS}$	0.35[c]	0.14[c]	0.07[c]	0.22[c]	0.4[c]
$AF_{ef,SAS}$	4.71	10.48	95620650	2744.83	6893.5
BBB transport (European Medicines Agency, 2021b, 2021a, 2020)					
P-gp	substrate	substrate	NA	substrate	not substrate
BCRP	not substrate	not substrate	NA	substrate	not substrate
ENT1	NA	NA	NA	substrate	NA
ENT2	NA	NA	NA	NA	substrate
CNT1	NA	NA	NA	not substrate	substrate
CNT2	NA	NA	NA	not substrate	substrate
CNT3	NA	NA	NA	substrate	substrate

Dosing (European Medicines Agency, 2021a, 2021b; U.S. Food and Drug Administration, 2020)					
Dose (mg)	300	200 + 100	NA	NA	800[d]
Dosing frequency (day^{-1})	twice	once	NA	NA	twice
Treatment duration (days)	5	5	NA	NA	5
Administration route	oral	IV	NA	NA	oral
Efficacy					
EC_{50} (delta) (uM)	0.076 (European Medicines Agency, 2021b; Rosales et al., 2022)	0.071 (European Medicines Agency, 2020; Rosales et al., 2022)	NA	0.86 (Vangeel et al., 2022)	1.43 (European Medicines Agency, 2021a; Rosales et al., 2022; Vangeel et al., 2022)
EC_{90} (delta) (uM)	0.149 (European Medicines Agency, 2021b; Rosales et al., 2022)	0.1455 (European Medicines Agency, 2020; Rosales et al., 2022)	NA	NA	4.65 (Rosales et al., 2022)
EC_{50} (omicron) (uM)	0.02 (Rosales et al., 2022)	0.02 (Rosales et al., 2022)	NA	0.5 (Vangeel et al., 2022)	0.25 (Rosales et al., 2022)
EC_{90} (omicron) (uM)	0.05 (Rosales et al., 2022)	0.09 (Rosales et al., 2022)	NA	NA	>10 (Rosales et al., 2022)

[a]Predicted values using the brain exposure efficiency score (Gupta et al., 2020)

[b]Kp value was calculated based on mouse brain homogenate (Painter et al., 2019) and was corrected to $Kp_{uu,BBB}$ accounting for the plasma and brain binding and brain pH differences

[c]assumed the same as $Kp_{uu,BBB}$

[d]Molnupiravir dose in the model simulations was performed in units of molarity to account for the difference of molecular weight between Molnupiravir and its metabolite EIDD1931.

MW: molecular weight, LogP: octanol-water partitioning, pK_a: acid dissociation constant, pK_b: base dissociation constant, CL_{cen}: drug clearance from central plasma compartment, $Q_{cen-per}$: Drug clearance between central and peripheral plasma compartments, V_{cen}: volume of central plasma compartment, V_{per}: volume of peripheral plasma compartments, Ka: absorption rate constant, D1: estimated duration, IIV: interindividual variability, fu,p: plasma unbound fraction, Kp_{uu}: unbound drug concentration ratio, $AF_{ef/in}$: asymmetry factor efflux/influx, P-gp: P-glycoprotein, BCRP: breast cancer receptor protein, ENT: equilibrative nucleoside transporters, CNT: concentrative nucleoside transporter, $EC_{50/90}$: drug concentration for 50%/90% efficacy, NA: not available